Assessing fine motor skills of children through sensor data and game state information

Jörg Sander
jorg.sander@toologic.com

Antoine de Schipper
a.w.de.schipper@hva.nl

Svetlana Mironcika
svetlana.mironcika@gmail.com

Ben Kröse
b.j.a.krose@hva.nl

1 Introduction

Children's activity levels have decreased over the past 25 years [1]. The amount of physical activity in the pre-school and toddler period is associated with the development of motor skills [3, 4]. Less physical active children engage themselves less in new activities that challenge their motor development. Consequently, the motor development is delayed. In Amsterdam alone the percentage of children with a delay in gross motor development is about 15% and this number increases [2].

In order to counter these developments it would be beneficial if the early detection of delayed motor skill development in primary school children could be facilitated with so called *smart play sets* that can be used in physical education. These play sets are capable to provide a high level diagnosis through analyzed sensor data (e.g. accelerometer or gyroscope) and possibly engage children in physical activities that are fun to do and offer relevant exercises for care and cure. In addition close monitoring of fine motor development could benefit both teachers to correctly identify the next learning step, as the child, in being engaged in a more optimal learning situation.

This article describes the experiments that were conducted in order to assess the motor skills of 6 to 7 years old children (hereafter referred to as children or toddlers) by means of an already developed toy called *futuro cube*[1]. The underlying assumption is that the sensor data and the game state information (description of an object at a given point in time in a game e.g. number of errors, level of difficulty, scores) that the futuro cube provides can be used to evaluate the fine motor skills of children that are necessary in many tasks in the primary school setting for example write, draw, puzzle or craft.

As a first step, the goal was to investigate the feasibility of this assumption and more specific the following research questions were addressed:

1. How accurately can the development of motor skills of children be estimated from the sensor data and game state information of the futuro cube?
2. What features might prove most sensitive to determine differences in motor capacity of children?

In order to explore these questions sensor and game state data was collected while two groups of children (one with delayed and the other with normal developed motor skills) were playing a game on the futuro cube. Features were extracted from the experimental data and a ranking algorithm was applied to generate a list of most sensitive features. In order to reduce the dimensionality of the data the performance of 4 different classifiers was evaluated on different ranked feature subsets. From the results it can be carefully concluded that it is possible to differentiate between children with normal and delayed fine motor skill development by means of a machine learning classifier that uses features extracted from the sensor and game state data.

[1] http://www.futurocube.com/

project AI (2016), SmartPlaySets, University of Amsterdam.

Figure 1: futuro cube

2 Related work

This section presents related work on automatic assessment of motor functions from sensor data collected during predefined motor skill assessment tasks. Previous research on quantitative assessment of motor abilities was mostly done on the topic of wearable technology in physical medicine and rehabilitation where subjects were suffering from severe motor impairments e.g. stroke survivors [12] or cerebral palsy [4].

In most related work, the goal was to assess motor skills with either signal processing or machine learning. The ground truth was obtained by experts' ratings or standard clinical rating scales. Using machine learning, the most common approach is to extract features from sensor data and apply a feature selection algorithm in order to reduce the dimensionality of the data. Finally one or more classification algorithms [11] are trained, validated and tested on the available data in order to assess their generalization performance.

With such a machine learning approach motor recovery of stroke survivors has been assessed using accelerometers attached to different positions of the patient's affected arm [12, 13]. Similarly, authors [14, 15] extracted statistical features from accelerometer data to predict motor function scores during different tasks. They were able to predict the scores with an error of 10%.

In [16] a post-stroke patient performed the Wolf Motor Function Test (WMFT) while being equipped with a single inertial measurement unit (IMU) on her wrist. The goal was to distinguish the movements between the affected and unaffected arm of the patient by means of a Naive Bayes classifier that used calculated features from the sensor data.

Zhang et al. [17] provided a fine-grained assessment of motor skills by capturing detailed patterns contained in the patients' movements. They used Dynamic Time Warping to compare movement trajectories of the affected and unaffected arm which embarks on a different motor skill assessment technique than building mapping functions that correlate sensed movement signals to expert or clinical rating scales.

The work presented in this article differs from previous research on quantitative assessment of motor abilities using sensor data in that the children participating in the experiments here do not suffer from severe motor skill impairments due to (birth) injuries. In addition the fine motor abilities of these toddlers were not pre-assessed with standard clinical rating scales. It is assumed that the differences in fine motor skills between these children are more fine-grained compared to the severe impaired children or adults participating in previous research.

Another difference with preceding experiments lays in the fact that the analysis presented here will include so called *game state* features e.g. an error measure that will quantify how accurately a child can perform the predefined task.

3 Methods

3.1 Approach

Jörg: I decided to phrase a high level approach of the experiments in the end of the introduction and therefore suggest that we skip the paragraph below that describes the same again.

In order to investigate the research questions that were addressed in the introduction, sensor and game state information was collected while children were playing a game on the futuro cube. The

Table 1: Details on participating children

ID	Age [years]	Gender	Handedness	Assessment
1	7	Boy	Right	delayed fine motor skill development
2	7	Boy	Left	delayed fine motor skill development
3	7	Boy	Left	delayed fine motor skill development
4	7	Girl	Right	
5	6	Boy	Right	delayed fine motor skill development
6	7	Girl	Right	
7	7	Girl	Right	
8	7	Girl	Right	delayed fine motor skill development
9	7	Girl	Left	

sensor data was used to extract time and frequency domain features. After a feature ranking process the remaining attributes were utilized to train and validate four different classification algorithms that learnt to assess the child's motor skill development. The extracted game state information was intended to give an indication of how well the children were able to play the game. Unfortunately due to a design flaw this information must be treated very carefully.

3.2 Experimental design

A total of 9 children, age 6 to 7 years, from a primary school in Amsterdam participated in the experiments. All children were assessed before the study by certified physical education teachers and 5 of them were classified as having developmental delayed fine motor skills (e.g. difficulties during handwriting). All characteristics of the participants can be found in table 1.

Each child performed 6 predefined motor tasks on 4 different toys[2] during the experiments. Children were tested individually for approximately 30 minutes and started with the futuro cube. The children were carefully instructed before performing the game once (without a training phase). Data collection started synchronously with the actual game. At the end of the experiment the child had to evaluate the different games by means of a smiley scale rating specifically developed for children.

3.3 Specifications of accelerometer meter and sensor data

The experimental data is collected from a 3-axial accelerometer (LIS3DH [3]) that is built into the *futuro cube* game device.

The built-in accelerometer uses a scale of $\pm 8g$ with a resolution of ± 2048 (where $1g \approx 256$) and is capable of measuring accelerations with output data rates from 1 Hz to 1.25 kHz. For each of the 3-axis the data output is 16 bit.

The following pre-processing is applied to the raw sensor signal in the cube before it is available in the *game software*:

- the signal is *right shifted* by four bits in order to attenuate high noise;
- a moving average filter of size four is applied to the signal;
- the filtered signal is passed to the *game software* every 8 ms.

Therefore the accelerometer data available in the game software has a maximum sampling frequency of 125 Hz.

3.4 Game device

The futuro cube uses vibration, audio and colorful LEDs to interact with the player. A foto of the cube is shown in figure 1. It uses a low energy communication protocol to wireless exchange information

[2]other game devices used during the experiments were: building blocks, balance boards, agility ladder

[3]`http://www.st.com/content/st_com/en/products/mems-and-sensors/accelerometers/lis3dh.html`

with a computer or another cube. Each site of the cube is divided into nine squares, containing a LED each that can be identified by a specific *index*, *side* and *square* number (a map of the cube is shown in figure 3).

3.5 *Roadrunner* game

The futuro cube can be programmed by a simple, typeless 32-bit language called *PAWN*[4]. The company that developed the futuro cube delivers a couple of APIs written in PAWN that facilitate the creation of new games. For this work a game application was scripted (referred to as roadrunner hereafter) to challenge and assess the bimanual speed and precision of the child.

The child has the task to pursue a white spot (hereafter referred to as *walker*) that moves over the surface of the cube. The player has to make sure that the walker is always on top of the cube.

The walker can move one step in three different directions forward, forward right and forward left. Steps performed by the walker can only be made to adjacent cube squares. The game is based on the assumption that it will be more difficult for the child to follow the walker if the delays i.e. intervals between the steps will decrease during the game. It should be obvious that the degree of difficulty of the game increases with shorter step-change perturbations.

The game uses a series of three levels of increased difficulty (referred to as *degree of difficulty* hereafter). A game lasts for 120 seconds and therefore each degree has a duration of 40 secs. The delay between steps at degree 2 and 3 is 80% resp. 70% of the delay used at degree 1. A step in one of the three possible directions is chosen randomly using uniform probabilities.

Although the game software provides a sampling frequency of 125 Hz the experimental setup could only capture samples with a frequency of approximately 20.8 Hz due technical limitations. Figure 9 illustrates the capturing of the accelerometer data during the experiments before they are being analyzed.

4 Data Analysis

The data analysis used accelerometer and game state data that were collected for each game performed by a child. All mathematical calculations in this study were performed using Python 2.7 with Numpy module 1.11.1.

The accelerometer data was digitally low-pass filtered with a cutoff frequency of 8 Hz to remove high frequency noise. [18] showed that few observable harmonics of volitional movement exist beyond 10 Hz. An example of a filtered 3-axial accelerometer signal is shown in figure 2.

Figure 2: Example of 8 Hz low-pass filtered accelerometer signal

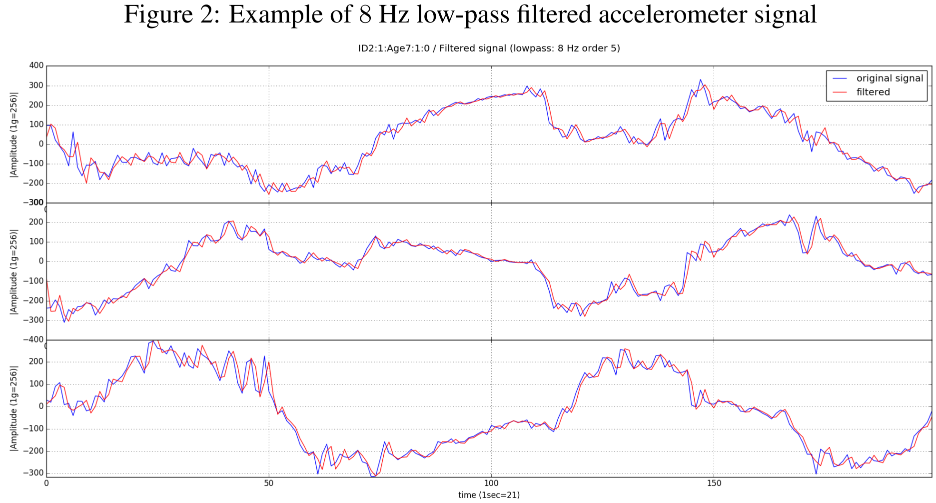

[4] http://www.compuphase.com/pawn/pawn.htm

For the further analysis the signal magnitude was calculated for each sample. The term *Movement Intensity* (MI) was coined in [5] and will be used here instead of signal magnitude. The MI was calculated as follows,

$$MI(t) = \sqrt{a_x(t)^2 + a_y(t)^2 + a_z(t)^2} \tag{1}$$

with $a_x(t)$, $a_y(t)$ and $a_z(t)$ being the acceleration measured on the x-axis, y- and z-axis, respectively at time t. The movement intensity is invariant to the the sensor's orientation in the game device.

For each child the accelerometer data was first segmented into 3 epochs of 40 seconds that coincide with the 3 degrees of difficulty of the game, before the features were extracted and computed for each epoch (the terms segment and epoch will be used interchangeably). Figure 8 visualizes the pre-processing pipeline of the accelerometer data.

4.1 Feature extraction

Time domain

Statistical & envelope metrics

Simple statistical and envelope metrics (e.g. minimum, range and mean) can be used to extract basic signal information from raw sensor data. These techniques were often used in practical activity recognition algorithms [6] as well as in motor skill assessment experiments [12, 13]. A list of all the features that were calculated in the time domain are shown in Table 2.

The mean movement intensity is frequently used as a feature in rehabilitation [11] and activity recognition [19]. In clinically environments, it is related to translational movements in space and can be used to detect postural transitions [5].

Common measures of smoothness of movement are jerk measures [7] and spectrum-based measures [8] (e.g. power spectrum entropy). This study calculated both measures and used a feature ranking algorithm to obtain their predictive power. Based on the work of [7] the mean squared jerk (MSJ) was calculated which is a dimensionless jerk measure

$$MSJ = \frac{1}{t_2 - t_1} \int_{t_1}^{t_2} \left(\frac{da}{dt}\right)^2 dt \tag{2}$$

where $\frac{da}{dt}$ denotes the time derivative of the movement intensity and t_1 and t_2 denote the begin respectively end of the time interval over which the mean was calculated. A simple 1D derivative filter was used to compute the change of movement intensity between successive samples.

Table 2: Features extracted from the time domain

No.	Feature
1	Minimum MI
2	Maximum MI
3	Mean MI
4	MI variation (standard deviation)
5	Median MI
6	Range of MI
7	Root mean squared MI
8	Mean squared jerk (smoothness)

Frequency domain

Before calculating the frequency domain features a Hamming window function was applied to the MI in order to alleviate spectral leakage. The Fourier Transform (FT) of the signal was calculated with a fast Fourier Transform (FFT) algorithm. The frequency spectrum reflects the frequencies at which the movement was performed. Table 3 shows the list of features that were calculated in the frequency domain.

DC component

The DC component is the first coefficient in the spectral representation of a signal and represents the average amplitude value of the signal in the time domain. It is used as a signal characteristic in several activity recognition approaches [19].

Dominant frequency

The dominant frequency of the performed motor task was calculated as the frequency associated with the highest energy of the FT acceleration signal (excluding the DC component).

Spectral energy

The spectral energy of the signal can be computed as the squared sum of its spectral coefficients normalized by the length of the sample window (i.e. the length of the epoch). The DC component is generally excluded from this calculation. The formula for the calculation of the spectral energy is outlined in equation (4).

Table 3: Features extracted from the frequency domain

No.	Feature
9	DC component
10	Dominant frequency
11	Spectral Energy
12	Power spectral entropy

Power spectral entropy (PSE)

Based-on the Shannon information theory the information entropy of the power spectrum is called power spectral entropy (PSE) which can be interpreted as is a complexity measure for an uncertain system [24]. For example [19] have used the PSE to distinguish between activities with similar energy levels. The calculation of the PSE is outlined in [24] and can be summarized as:

Assuming that a random variable X represents the states of an uncertain system, where $X = \{x_1, x_2, \ldots x_n\}$ and $n \geq 1$. The corresponding probability is $P(X) = \{p_1(x_1), p_2(x_2), \ldots p_N(x_N)\}$ and $0 \leq p_i \leq 1, i = 1, 2, \ldots N$ under the constraint that $\sum_{i=1}^{N} p_i(x_i) = 1$. The information entropy of the system can be expressed as

$$H = -\sum_{i=1}^{N} p_i \log p_i \tag{3}$$

The time-series signals (the different states of X over time) become a power spectrum by the FFT transform.

1. The Discrete Fourier Transform $X(\omega_i)$ of a signal can be obtained by FFT where ω_i is the frequency point of the number i;
2. Calculate the power spectral density (PSD)
$$\hat{P}(\omega_i) = \frac{1}{N}|X(\omega_i)|^2 \tag{4}$$
3. Normalize $\hat{P}(\omega_i)$, and obtain the PSD distribution function
$$p_i = \frac{\hat{P}(\omega_i)}{\sum_i \hat{P}(\omega_i)} \tag{5}$$
4. Then substitute p_i into the equation (3) for the information entropy of the system.

Game state features

Degree of difficulty

As mentioned above the roadrunner game was composed of 3 degrees of difficulty. The degree d with $d \in \{1, 2, 3\}$ was captured together with all other features in order to use this information in the analysis (e.g. to detect the step-changes).

Figure 3: Visualizing the calculation of the error measure

Cursor	Walker	dx	dy	Euclidean distance	Remark
		-1	4	sqrt(17)	
		0	0	6	Opposite site of cursor fixed value
		-3	-1	sqrt(10)	
		1	-1	sqrt(2)	

Note, this feature was not captured explicitly in the current work. As mentioned before, the game was segmented in fixed epochs of 40 secs with increased degree of difficulty. Therefore the step-changes could be derived afterwards in the analysis. In future experiments the degree of difficulty of an epoch will be a randomized property and needs to be collected explicitly during the experiment.

Error measure

In order to measure how accurately a child can pursue the optimal trail of the walker, an error measure was defined. Figure 3 visualizes the unfolded cube and illustrates four possible situations that exemplifies the calculation of this error measure. The so called *cursor* (the yellow circle at position (0,4)) is defined as the gravity cursor that indicates the top of the cube and is calculated by means of the acceleration data provided by the system[5]. As explained before the goal of the game is to keep the walker exactly on the same position (i.e. square) as the gravity cursor.

The software of the cube provides a function that calculates the distance of the cursor and the walker in the xy-plane at time t denoted as $\Delta x(t)$ and $\Delta y(t)$ where $\Delta x, \Delta y \in \mathbb{Z}$.

The experimental data contained the sum

$$d(t) = \Delta x(t) + \Delta y(t) \tag{6}$$

for each timestamp t. Obviously this should have been the sum of the absolute values $|\Delta x(t)| + |\Delta y(t)|$. Besides, after the experiments it was discovered that the cube software assigns a value of zero to both measures in case the cursor and the walker are located on opposite sides of the cube. Therefore the data w.r.t. the error measure was expected to be unreliable. Nevertheless the sum of

[5] this location was not visible for the player.

squared errors (SSE) was calculated for each segment

$$SSE = \sum_{t=1}^{T} d(t)^2 \tag{7}$$

where T denotes the length of a time segment (in our case 40 seconds).

Note, the upcoming experiments will capture the separate $\Delta x(t)$ and $\Delta y(t)$ values. As a final error measure the Euclidean distance will be calculated between the cursor and the walker in $\mathbb{R}^2$.

$$d(t) = \sqrt{|\Delta x(t)|^2 + |\Delta y(t)|^2} \tag{8}$$

Table 4: Game state features

No.	Feature
13	Sum of squared errors
14	Maximum overshoot error
15	Error correction measure

A fixed error value of 6 will be assigned to all situations in which the walker and the cursor are located on opposites sides of the cube. Naturally the measure is equal to zero in case the cursor and walker are exactly positioned on the same location. The measure is maximally in case both objects are positioned on opposite sites of the cube.

Error correction due to step-change perturbations

Note, the features described in this section were not calculated in the current work. They are based on the error measure outlined in the previous section. These features are intended to be used in future work.

In [20] Bavassi et al. used among others small step-change perturbations in a finger-tapping task that revealed inherent nonlinearities in the underlying error correction mechanism. The roadrunner game with its transition points between game levels can be interpreted as step-change perturbations to which the child will react with a sensorimotor synchronization response in order to align her movements to the altered speed of the game.

Research has shown [20, 21] that human motor response to a step-change exhibit considerable overshoot[6] before approaching the new baseline. Another interesting finding from the step-change perturbations is that the overshoot is only displayed for positive perturbations, i.e., when the period of the sequence is increased but not when it is decreased [21].

Based on these findings the following 2 features were designed

1. *Maximum overshoot error (MOE)*, maximum error in the 100ms interval following the step-change perturbation where

$$MOE = \max\left[d(t_0), d(t_1)\right] \tag{9}$$

   and $\Delta t = t_1 - t_0 \approx 100$ms;

2. *Error correction measure (ECM)*, sum of errors until the new baseline (error) is achieved,

$$ECM = \int_{t_0}^{t_1} d(t)dt \tag{10}$$

   and $\Delta t = t_1 - t_0 \approx 2000$ms[7].

The design of these features hinge on the assumption that children with delayed fine motor skill development will react less optimal i.e. slower to the step-change perturbations than children without

[6] to be explained

[7] validate and discuss with Antoine which time interval would be appropriate

fine motor skill deficiencies and will therefore exhibit significantly larger overshoots and error correction values[8].

Table 4 lists all game state features.

Feature ranking and selection

Feature selection is widely used in machine learning before performing tasks like classification, clustering and recognition. Redundant and irrelevant features cannot improve the learning accuracy and even deteriorate the performance of the learning models. Therefore, selecting an appropriate and small feature subset from the original features reduces the dimensionality of the data and contributes to accomplish the learning tasks effectively. The aim of feature selection is to find a feature subset that has the most discriminative information from the original feature set. This work performed feature ranking and selection by means of a two step approach.

In the first step the optimal feature ranking was determined by the ReliefF algorithm [9] which is an extension of the original Relief algorithm proposed by [10], that has been designed for multiclass problems.

The algorithm aims at estimating the quality of features according to how well their values separate the instances according to their distance in the problem space [9]. Given a randomly selected instance, the algorithm searches for the k nearest neighbors from the same class and k nearest neighbors from each of the other possible classes. Based on which class do the neighbors belong to, the algorithm updates the feature quality information by increasing its value if the feature separates instances with different classes well and by decreasing its value in the opposite scenario. The process of random instance selection is repeated for several times, where the number of iterations is pre-chosen by the user. The main property of the ReliefF algorithm is that the quality estimation of a single feature implicitly depends on the context of other features, meaning that the method detects their interaction as well [23].

In a subsequent step a sequential backward selection (SBS) process was performed that uses the features to train a specific classifier and evaluate the N_i ranked features in subset $\mathcal{F}_{N_i}$ where $N_i \in \{N, N-1\ldots,1\}$ denotes the number of features in a subset (with $i \in \{1,\ldots,N\}$) and N denotes the total number of ranked features. The subset $\mathcal{F}_N$ contained all N top ranked features and each successive set contained the top N_i ranked features where the lowest ranked feature from the previous set was omitted. The performance of a classifier was evaluated on each feature set (in reduced order) by means of the validation accuracy percentage that was derived by performing a four-fold cross-validation.

The following classifiers where trained and evaluated during the backward selection process

1. Support Vector Machines[9] (SVM);
2. Random Forest (RF);
3. Extreme Gradient Boosting machine (XGB);
4. Gaussian Naive Bayes (GNB).

The analysis was implemented using the machine learning toolbox *scikit-learn* release 0.18 and the ReliefF implementation from [23].

5 Results

This section presents the preliminary results of the experiments and data analysis outlined above. Results are described for 2 scenarios. In scenario (1) the game state feature *sum of squared errors* was excluded in the analysis whereas in scenario (2) this feature was a member of the feature set to be evaluated. As illustrated earlier the error measure was supposed to be unreliable due to the way it was captured.

[8] tiny synchronization errors or small differences between the interstimulus interval and the interresponse interval could rapidly accumulate and make the responses drift away from the stimuli, as it is that children with serious fine motor skill deficiencies could possibly not adjust to the perturbations

[9] using a non-linear RBF kernel

Scenario (1) contained 12 features and Table 7 shows their rank determined by the ReliefF algorithm. The power spectral energy which is a measure of randomness and movement smoothness is the best ranked feature followed by the spectral energy and the DC component. The best ranked time domain feature is the mean squared jerk which is a measure of movement smoothness. It is subsequently pursued by the root mean squared movement intensity value which is a measure for the dynamic energy of a movement [12].

Figure 4 shows the standardized power spectral energy scores for each child (for one game of roadrunner) averaged over the game epoch i.e. over the time window of a constant level of difficulty. A dotted line connects the successive scores of one child in order to visualize the change over time.

Using the ranked feature list of scenario (1) as input for the backward feature selection process that uses the accuracy scores of the four mentioned classifiers as evaluation measure, the results indicate that the Gaussian Naive Bayes classifier with an accuracy score of 77% and a standard deviation of 0.185 attains the best performance on the set of 5 best ranked features shown in table 7.

The other 3 classifiers obtain their best discriminatory performance equal to 70% with a subset of 4 top ranked features as can be seen in table 5.

Scenario (2) included as 13^{th} feature the SSE which quantifies how accurately a child can perform the predefined task. In the feature ranking obtained with the ReliefF algorithm this feature claims the highest rank. Figure 5 presents per epoch the standardized SSE measures for each child where a dotted line connects the consecutive scores of the player. The results of the feature ranking and backward feature selection process for scenario (2) are shown in table 6 resp. figure 8.

Table 5: Top accuracy scores of classifiers during backward feature selection - scenario (1)

Rank	Classifier	Max accuracy [%]	2σ	# of top ranked features
1	GNB	77	0.37	5
2	RF	70	0.38	4
2	SVM	70	0.38	4
2	XGB	70	0.38	4

Table 6: Top accuracy scores of classifiers during backward feature selection - scenario (2)

Rank	Classifier	Max accuracy [%]	2σ	# of top ranked features
1	RF	77	0.33	8
1	SVM	77	0.33	8
1	XGB	77	0.33	8
2	GNB	73	0.36	6

Table 7: Top ranked features by the ReliefF algorithm - scenario (1)

Rank	Feature
1	Power spectral entropy
2	Spectral energy
3	DC component
4	Mean squared jerk
5	RMS
6	Range
7	Median
8	Standard deviation
9	Mean
10	Max
11	Min
12	Dominant frequency

Table 8: Top ranked features by the ReliefF algorithm - scenario (2)

Rank	Feature
1	Sum of squared errors
2	Power spectral entropy
3	Spectral energy
4	DC component
5	Mean squared jerk
6	RMS
7	Range
8	Median
9	Standard deviation
10	Mean
11	Max
12	Min
13	Dominant frequency

6 Discussion

From the results of the experiments it can be carefully concluded that it is possible to estimate expert ratings of fine motor skills of children by means of a classifier algorithm that uses time and frequency domain features extracted from accelerometer data of the futuro cube. Although the accuracy of the best classifiers is promising its uncertainty ($\sigma \approx 0.185$ for scenario 1 and $\sigma \approx 0.165$ for scenario 2) is large. It must be mentioned that the classifiers are most certainly overfitted due to the limited amount of data that was available for the analysis. The generalization performance of the classifiers was never genuinely assessed because all data was used in the 4-fold cross-validation procedure. Future experiments must evaluated the reliability and validity of the described approach across a sufficiently large population of children.

The binary classification of motor skill competencies of children is a good starting point but this level of granularity is too low. Subsequent work will have to estimate more fine grained expert ratings or must use standard motor skill assessment tests that deliver a more precise estimate of the children's motor skills that can be used for training a machine learning algorithm (e.g. the Movement Assessment Battery for Children, MABC-2).

The results of scenario (1) reveal that especially frequency domain features prove to be sensitive to determine changes in motor capacity of children. This is interpreted to be in line with previous research that identified these features to measure movement coordination and smoothness [8].

Although a flaw was discovered in the calculation of the error measure, the results of scenario (2) point in the direction that well designed game state features could be very powerful predictors of fine motor skill capacities. Despite the unreliability of the error measure it was the most predictive feature in scenario (2) and therefore future experiments have to make sure that the game state features described in this work will be carefully designed and evaluated.

In the experiments conducted the children had no training time in order to get used to the working of the futuro cube and the roadrunner game in particular. Most certainly this has influenced especially the first epoch of the game when the children needed to learn how they could steer the cube in the desired position. Due to the already mentioned sparsity of the data it was decided to use all available data.

The results of the feature selection process reveal that especially most of the statistical envelop features from the time domain are *misleading* for the classification performance of the algorithms. The reasonable accuracy scores of the simple and computationally inexpensive Naive Bayes algorithm with only 5 features is a promising result. The final goal is to use streaming data from the futuro cube to incrementally update the classifier model (i.e. active learning) in order to feedback information to the cube software in real-time that adjusts the level of difficulty of the game resulting in a more optimal learning situation for the child.

Figure 4: Standardized power spectral energy scores per child/window

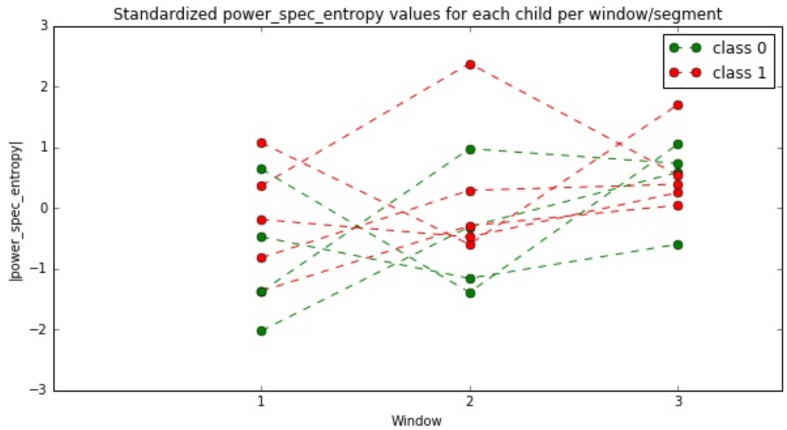

Class 0: normal motor skills / Class 1: delayed motor skills

Figure 5: Standardized error (measure) scores per child/window

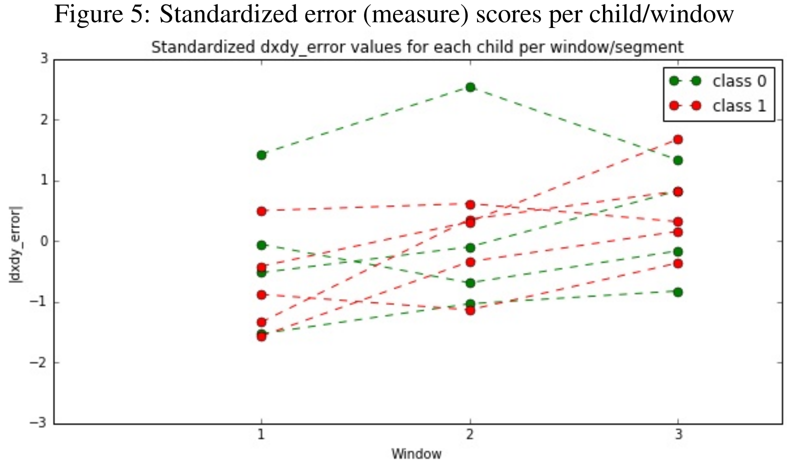

Class 0: normal motor skills / Class 1: delayed motor skills

Figure 6: Results sequential backward selection process (error bars represent 2σ) - scenario (1)

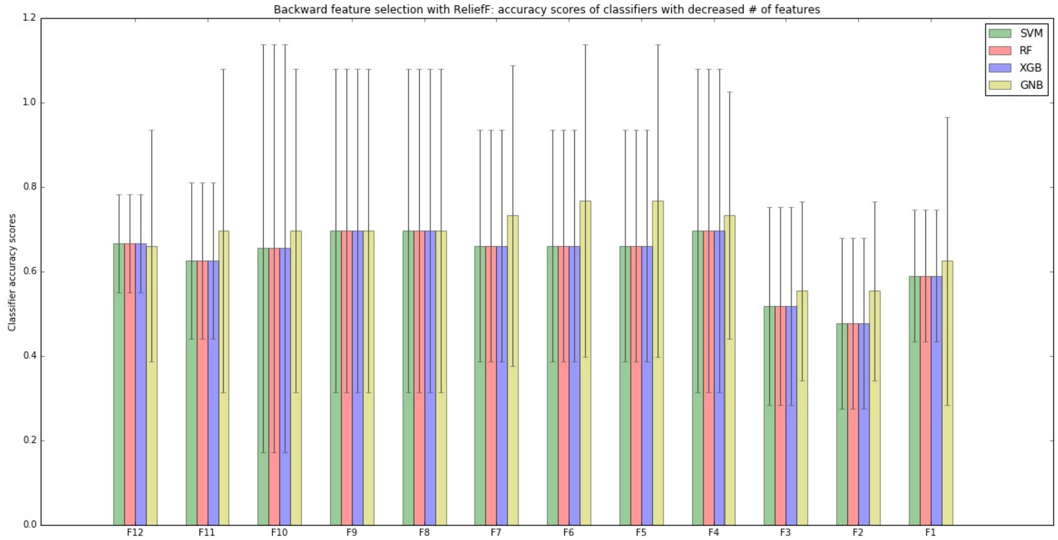

Figure 7: Results sequential backward selection process (error bars represent 2σ) - scenario (2)

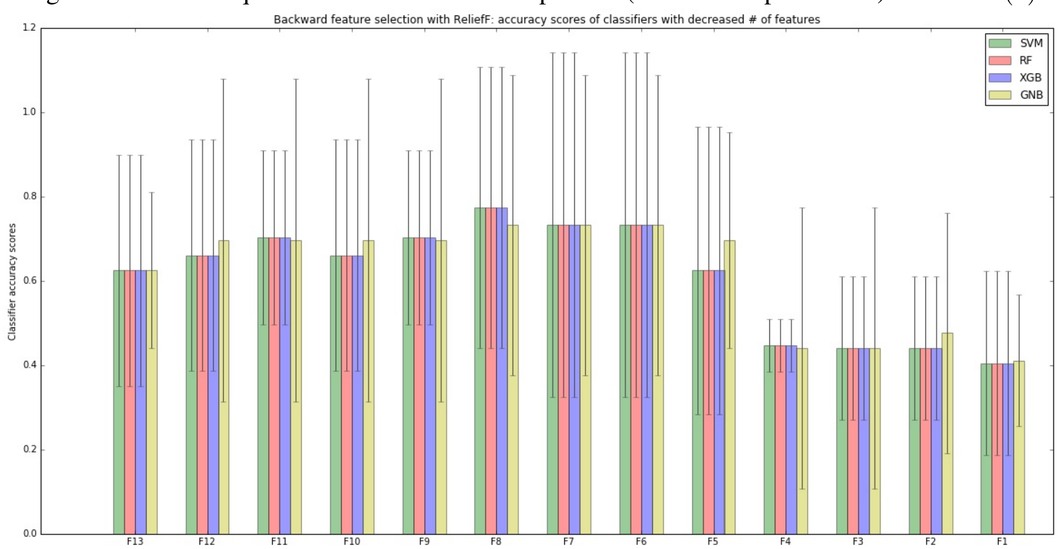

References

[1] Hildebrandt, V.H., A.M.J. Chorus, J.H. Stubbe, Trendrapport Bewegen en Gezondheid 2008/2009. 2010, TNO Kwaliteit van Leven: Leiden.

[2] Kurtz, L.A., Understanding motor skills in children with dyspraxia, ADHD, autism, and other learning disabilities. 2008, London: Jessica Kingsley Publishers.

[3] Fisher, A, et al., Fundamental movement skills and habitual physical activity in young children. Medicine and Science in Sports and Exercise, 2005. 37: p. 684 - 688.

[4] Cliff, DP, AD Okely, LM Smith, K McKeen, Relationships between fundamental movement skills and objectively measured physical activity in preschool children. Pediatr Exerc Sci, 2009. 21: p. 436 - 449.

[5] Strohrmann, Christina, et al. "Monitoring motor capacity changes of children during rehabilitation using body-worn sensors." Journal of neuroengineering and rehabilitation 10.1 (2013): 1.

[6] Kern N, Schiele B, Schmidt A (2007) Recognizing context for annotating a live life recording. Personal and Ubiquitous Computing 11(4):251–263

[7] Hogan N, Sternad D: Sensitivity of smoothness measures to movement duration, amplitude, and arrests. J Motor Behav 2009, 41(6):529–534.

[8] Kojima M, Obuchi S, Mizuno K, Henmi O, Ikeda N: Power spectrum entropy of acceleration time-series during movement as an indicator of smoothness of movement. J Physiol Anthropol 2008, 27(4):193–200.

[9] M. RobnikŠikonja and I. Kononenko, Theoretical and empirical analysis of Relieff and Relieff, Machine Learning 53(1–2) (2003), 23–69.

[10] K. Kira and L.A. Rendell, "A practical approach to feature selection," Ninth International Workshop on Machine learning, Aberdeen, Scotland: Morgan Kaufmann, 1992, pp. 249 - 256.

[11] Bonato P: Advances in wearable technology and applications in physical medicine and rehabilitation. J NeuroEng Rehabil 2005, 2:2.

[12] Patel S, Hughes R, Hester T, Stein J, Akay M, Dy J, Bonato P: Tracking motor recovery in stroke survivors undergoing rehabilitation using wearable technology. In Proceedings of the 32nd Annual International Conference of the IEEE EMBS: IEEE; 2010:6858–6861.

[13] Patel S, Hughes R, Hester T, Stein J, Akay M, Dy J, Bonato P: A novel approach to monitor rehabilitation outcomes in stroke survivors using wearable technology. Proc IEEE 2010, 98:450–461.

[14] Hester T, Hughes R, Sherrill D, Knorr B, Akay M, Stein J, Bonato P: Using wearable sensors to measure motor abilities following stroke. In Wearable and Implantable Body Sensor Networks, 2006. BSN 2006. International Workshop on: IEEE Computer Society; 2006: 4, pp. 5–8.

[15] Del Din S, Patel S, Cobelli C, Bonato P: Estimating fugl-meyer clinical scores in stroke survivors using wearable sensors. In Engineering in Medicine and Biology Society, EMBC, 2011 Annual International Conference of the IEEE: IEEE; 2011:5839–5842.

[16] Parnandi A, Wade E, Mataric M: Motor function assessment using wearable inertial sensors. In Engineering in Medicine and Biology Society (EMBC), Annual International Conference on: IEEE; 2010:86–89.

[17] Zhang M, Lange B, Chang CY, Sawchuk AA, Rizzo AA: Beyond the standard clinical rating scales: fine-grained assessment of post-stroke motor functionality using wearable inertial sensors. In International Conference of the IEEE Engineering in Medicine and Biology Society (EMBC); 2012.

[18] Hotraphinyo LF, Riviere CN. Three-dimensional accuracy assessment of eye surgeons. Proceedings of the 23rd annual international conference of the IEEE Engineering in Medicine and Biology Society, Vols 1-4. 2001;23:3458-3461.

[19] Bao, Ling. Physical activity recognition from acceleration data under semi-naturalistic conditions. Diss. Massachusetts Institute of Technology, 2003.

[20] Bavassi, M. Luz, Enzo Tagliazucchi, and Rodrigo Laje. "Small perturbations in a finger-tapping task reveal inherent nonlinearities of the underlying error correction mechanism." Human movement science 32.1 (2013): 21-47.

[21] Thaut, M. H., Miller, R. A., Schauer, L. M. (1998). Multiple synchronization strategies in rhythmic sensorimotor tasks: phase vs period correction. Biological Cybernetics, 79, 241–250.

[23] Randy Olson, (2016). ReliefF: First release [Data set]. Zenodo. http://doi.org/10.5281/zenodo.47803

[23] I. Kononenko and M. Kukar, Machine learning and data mining, Horwood Publishing, Chichester, UK, 2007.

[24] Zhang, Aihua, Bin Yang, and Ling Huang. "Feature extraction of EEG signals using power spectral entropy." 2008 International Conference on BioMedical Engineering and Informatics. Vol. 2. IEEE, 2008.

7 Appendix A

7.1 Flowchart of pre-processing steps

Please see figure 8 for a visualization of the pre-processing flow.

Figure 8: Pre-processing flowchart

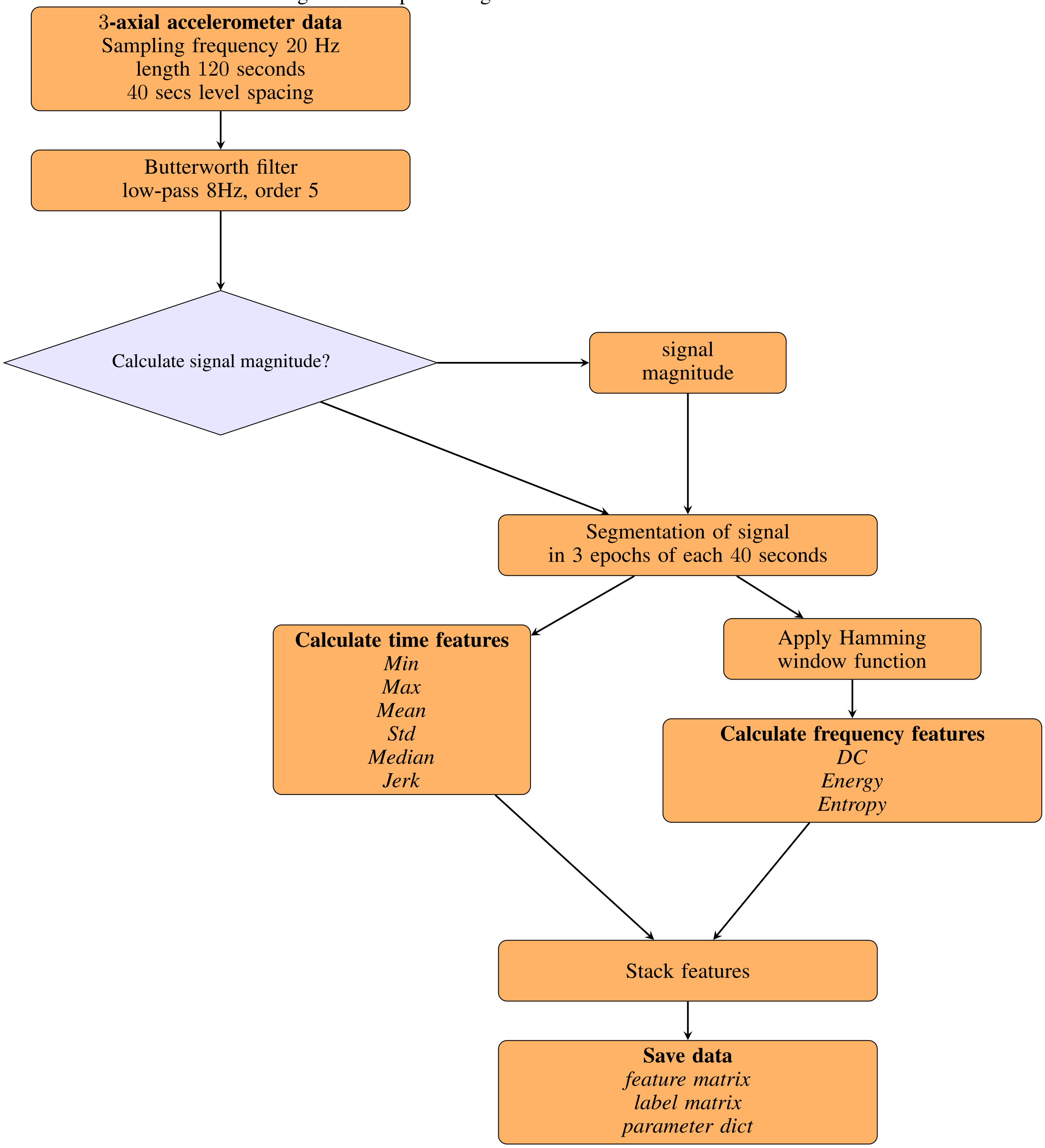

Figure 9: Flowchart of capturing accelerometer measurements

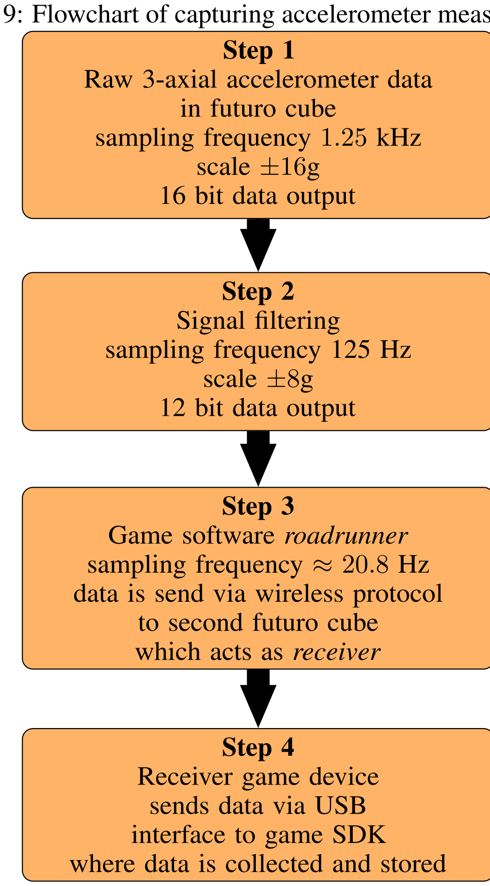

Figure 10: Demonstration of the cursor and walker LEDs on the futuro cube

The upper green LED indicates the cursor position and the lower bluish LED demonstrates the walker